Surface depinning of smectic-*A* edge dislocations

M. Slavinec,[1] S. Kralj,[1,2] S. Žumer,[2,3] and T. J. Sluckin[4]
[1]*Laboratory Physics of Complex Systems, Faculty of Education, University of Maribor, Koroška 160, 2000 Maribor, Slovenia*
[2]*Institute Jožef Stefan, Jamova 39, 1000 Ljubljana, Slovenia*
[3]*Department of Physics, Faculty of Mathematics and Physics, University of Ljubljana, Jadranska 19, 1000 Ljubljana, Slovenia*
[4]*Faculty of Mathematical Studies, University of Southampton, Southampton SO17 1BJ, United Kingdom*
(Received 18 April 2000; published 27 February 2001)

Using a Landau–de Gennes approach, we model the formation of an edge dislocation in a smectic-*A* cell initially in the bookshelf structure. The driving force is the mismatch between the layer thickness in a bulk smectic-*A* liquid crystal and that imposed by confining plates. The core structure of the dislocation is calculated taking into account spatial variations of the smectic translational order parameter. We numerically determine the critical condition for the surface-driven formation and depinning of the dislocation. By exploiting this phenomenon, we show how the value of the positional anchoring strength at the surface can be determined.

DOI: 10.1103/PhysRevE.63.031705 PACS number(s): 61.30.Jf, 61.72.Bb

I. INTRODUCTION

In bulk smectic liquid crystal [1] (LC), planar layers are characterized by the periodicity $q_b = 2\pi/d_b$. Within each layer, the distribution of a center of mass of a LC molecule exhibits two-dimensional (2D) liquidlike behavior. Different families of smectics are classified mainly according to orientational ordering of molecules within layers. In the simplest smectic-*A* (Sm*A*) phase, which is the subject of this study, the molecules are aligned along the layer normal. The essential features of this phase are covered by relatively simple models that also serve as a basis for understanding more sophisticated smectic phases, particularly concerning the layer structure.

The most energy-demanding deformations in smectic phases are those tending to expand or compress smectic layers. If, nevertheless, such deformations are *imposed*, a Sm*A* phase often responds by introducing a lattice of edge or screw dislocations [2]. In this way, strong smectic elastic distortions can be localized in finite regions in the form of dislocations. A typical example involves the various twist grain boundary [3] (TGB) phases, which have been widely studied recently [4,5]. In these phases, the imposed nematic twist distortion is localized in a lattice of screw dislocations.

The lattice of edge dislocations, which has been so far less studied [6], can be enforced in various ways. It may form as a response to a bend deformation in the nematic ordering. It may alternatively appear when some external potential enforces surface periodicity $q_s = 2\pi/d_s$ not equal to the bulk periodicity q_b. This is often the case when the smectic layers are stacked perpendicular to a confining surface, which enforces periodicity q_s. The apparent intrinsic surface periodicity [7] is usually attributed to a surface memory effect [8]. The surface is thought to retain the bulk periodicity that first appeared when the smectic phase condensed above the initially isotropic surface. In this picture, when the system is cooled gradually from the nematic phase, the surface periodicity q_s appears to resemble that periodicity q_b which is obtained at the nematic-smectic phase transition.

However, the bulk imposed stress established for $q_s \neq q_b$ can also be partially relaxed via other channels. We now list some of the most relevant scenarios in the so-called bookshelf smectic configuration, which plays an essential role in various electro-optical applications. In this structure, shown in Fig. 1, the smectic layers are perpendicular to the confining surfaces of the liquid-crystal cell. In this geometry, a mismatch between the bulk smectic wave number q_b and a surface wave number q_s imposed by the confining surface often appears. If the system remains in the bookshelf geometry, the stress is uniformly distributed across the whole cell of thickness L_x. Then if the stress exceeds some critical value (which is proportional to L_x^2 [6,9]), structural changes appear, enabling the elastic penalties to be localized. The equilibrium structure involves a balance between orientational and positional anchoring energy, nematic director bending, smectic layer compression, and smectic melting free-energy costs.

If $q_s < q_b$, the initial bookshelf structure usually deforms and a buckled *chevron* state appears [Fig. 2(a)]. The smectic layers form a V shape, meeting in the middle of the cell [6,9–11]. Tilting the layers reconciles the bulk and surface periodicities. If the layers are allowed to slip at the bounding plates, the smectic layers simply tilt to satisfy the positional boundary condition, resulting in the so-called *tilted* structure [Fig. 2(b)] [6,9,11]. In principle, however, one might also

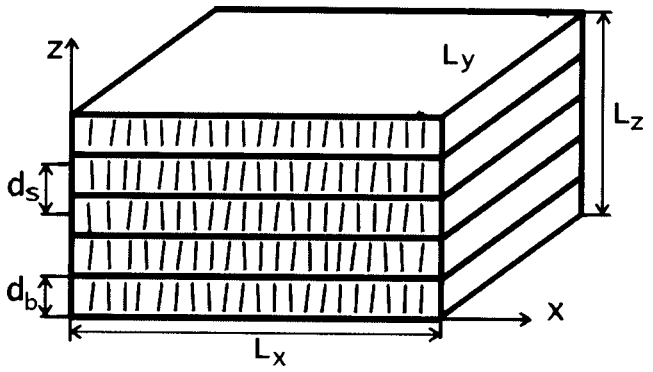

FIG. 1. The bookshelf structure and coordinate system of the problem.

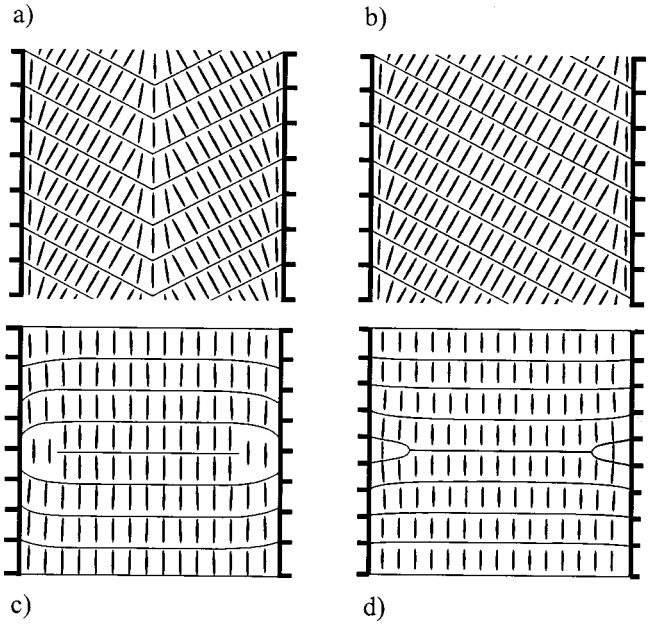

FIG. 2. For $d_s \neq d_b$, the bookshelf structure can become unstable with respect to the chevron (a), tilted (b), and dislocation (*c*,*d*) structure.

imagine that the surface and bulk periodicities could be reconciled by layer slippage without tilting the layers. There are then two possibilities. For strong positional surface anchoring, a lattice of edge-dislocation lines [Figs. 2(c) and 2(d)] might form at or close to the walls. Alternatively, for weak positional surface anchoring, there might be some degree of layer slippage at the interface. In practice, this will only occur [6] close to the nematic-smectic phase transition or in the presence [12] of an external electric or magnetic field supporting the bookshelf arrangement.

However, when $q_s > q_b$, the mismatch can no longer be accommodated by a layer tilt. The accommodation must now occur either through layer slippage or by creating a dislocation structure.

In the phenomena described above, edge dislocations play the central role. The structure of a single edge dislocation has already been studied theoretically using continuum-type approaches [1,13]. These studies have been carried out in the constant smectic order-parameter approximation and require the introduction of a cutoff radius. In this paper, we need to develop a description of the surface-induced formation of an edge dislocation in the Sm*A*LC phase that also allows spatial variation of the smectic order parameter.

The plan of the paper is as follows. In Sec. II, we introduce the model. In Sec. III, we study the surface-driven formation of an edge dislocation and its depinning from the substrate. We propose an experiment to determine the value of the surface positional anchoring. The results are summarized in Sec. IV.

II. MODEL

A. Free energy

We use the Landau–de Gennes approach [1,3,6], in which ordering in the Sm*A* phase is described by the nematic director field **n** and the smectic complex order parameter $\psi = \eta e^{i\phi}$. The uniaxial vector **n** points along the local average orientation of rodlike LC molecules, η is the amplitude of the smectic density wave ($\eta = 0$ in the nematic phase), and the phase factor ϕ determines the position of the smectic layers.

It is convenient to write the free energy F of the confined liquid crystal as the sum of a homogeneous smectic contribution f_b, a nematic elastic contribution $f_e^{(n)}$, a smectic elastic contribution $f_e^{(s)}$, and a surface positional contribution $f_s^{(s)}$:

$$F = \int (f_b + f_e^{(n)} + f_e^{(s)}) d^3r + \int f_s^{(s)} d^2r, \tag{1}$$

where d^3r and d^2r denote, respectively, volume and surface integrations.

These contributions are given by [1,3,6]

$$f_b = \alpha \frac{T - T_{NA}}{T_{NA}} |\psi|^2 + \frac{\beta}{2} |\psi|^4, \tag{2a}$$

$$f_e^{(n)} = \frac{K_{11}}{2} (\nabla \cdot \mathbf{n})^2 + \frac{K_{22}}{2} (\mathbf{n} \cdot \nabla \times \mathbf{n})^2 + \frac{K_{33}}{2} (\mathbf{n} \times \nabla \times \mathbf{n})^2, \tag{2b}$$

$$f_e^{(s)} = \gamma_{\|} |(\mathbf{n} \cdot \nabla - i q_b) \psi|^2 + \gamma_{\perp} |(\mathbf{n} \times \nabla) \psi|^2, \tag{2c}$$

$$f_s^{(s)} = \frac{1}{2} W_p |\psi - \psi_s|^2. \tag{2d}$$

The material constants α and β determine the degree of ordering in the unconstrained bulk Sm*A* phase, T is the absolute temperature, and T_{NA} is the temperature of the bulk nematic-Sm*A* continuous phase transition. Below T_{NA}, the potential f_b enforces $\eta(T) = \eta_b = \sqrt{[\alpha(T_{NA} - T)]/\beta T_{NA}}$. The nematic splay ($K_{11}$), twist ($K_{22}$), and bend ($K_{33}$) elastic constants tend to establish homogeneous orientational ordering along the symmetry breaking direction. Close to T_{NA}, the twist and bend elastic constant exhibit an anomalous increase attributed to fluctuations in the smectic degree of ordering. The discussion of this anomaly will be postponed for future studies. The smectic compressibility ($\gamma_{\|}$) and bend ($\gamma_{\perp}$) elastic constants favor layer periodicity q_b and the nematic director orientation along the layer normal, respectively. In most cases, the ratio $\gamma_{\|}/\gamma_{\perp}$ is roughly proportional to the ratio between the length and width of a LC molecule [1]. In our calculations, we have used a nematic and smectic one-constant approximation, for which $K_{11} = K_{22} = K_{33} \equiv K$ and $\gamma_{\|} = \gamma_{\perp} \equiv \gamma$.

The smectic surface free-energy density is measured in terms of the positional anchoring strength W_p, tending to establish the smectic ordering $\psi_s = \eta_s e^{i\phi_s}$. In addition, we assume that the surface imposes strong tangential orientational anchoring, i.e., it enforces to **n** orientation perpendicular to the surface normal.

The functional (2) implicitly defines two lengths that play an essential role in our calculations. These are [1] the smec-

tic correlation length $\xi=\xi_0/\sqrt{1-(T/T_{NA})}$ with $\xi_0=\sqrt{\gamma/\alpha}$, and the surface positional extrapolation length $\zeta=\gamma/W_p$. For completeness, we define also the smectic penetration length $\lambda=\sqrt{K/\gamma\eta_b^2 q_b^2}$.

B. Parametrization and scaling

We perform calculations in the Cartesian-coordinate system (x,y,z) introduced in Fig. 1. The Sm*A* LC is restricted to a cell of width L_x with cell surface area $L_y L_x$. The layers are stacked along the z direction and the system is homogeneous in the y direction. The surface enforces tangential orientational anchoring (i.e., the easy axis of the orientational anchoring surface potential points along the z axis) and enforces periodicity $q_s=2\pi/d_s$ (i.e., $\phi_s=q_s z$). For numerical purposes, we introduce the phase slippage $\varphi(x,z)=q_s z-\phi(x,z)$. As z is increased at constant x, this quantity tracks the effective wave number of the smectic layers at x. If $d\varphi/dz=0$, then the layers are essentially entrained by the surface. The director field is parametrized as $\mathbf{n}=(\cos\vartheta,0,\sin\vartheta)$. The variational parameters of the model are thus $\vartheta(x,z)$, $\varphi(x,z)$, and $\eta(x,z)$.

We further introduce the reduced temperature $\tau=(T-T_{NA})/T_{NA}$, dimensionless stress parameter $\varepsilon=(d_b/d_s)-1=(q_s/q_b)-1$, scaled smectic order parameter $\tilde{\eta}=\eta/\eta_b$, and we define rescaled lengths and operators in units of d_b: $\tilde{x}=x/d_b$, $\tilde{y}=y/d_b$, $\tilde{z}=z/d_b$, $\tilde{\nabla}=d_b\nabla$. Subsequently, we drop the tildes.

In the dimensionless representation, we obtain the following expression for the dimensionless free energy $G=F/(L_y\gamma\eta_b^2)$:

$$G=\int\int dx\,dz\Big(\eta^2\{2\pi[\cos\vartheta(1+\varepsilon)-1]-\mathbf{n}\cdot\nabla\varphi\}^2+(\mathbf{n}\cdot\nabla\eta)^2+\eta^2|2\pi[\sin\vartheta(1+\varepsilon)]-\mathbf{n}\times\nabla\varphi|^2+|\mathbf{n}\times\nabla\eta|^2\Big)+\int\int dx\,dz\left[\frac{d_b^2}{\xi^2}\left(-\eta^2+\frac{\eta^4}{2}\right)+\frac{q_b^2\lambda^2}{2}|\nabla\vartheta|^2\right]+\int\frac{d_b}{2\zeta}|\eta-\eta_s e^{i\varphi}|^2dz. \tag{3a}$$

In our numerical calculations, we express the smectic order parameter as $\eta e^{i\varphi}=A+iB$, where $A=A(x,z)$ and $B(x,z)$ are real functions. In melted regions, this circumvents problems with the definition of φ when $\eta=0$. Using this representation, Eq. (3a) can be rewritten as

$$G=\int\int dx\,dz\left[\frac{d_b^2}{\xi^2}[(A^2+B^2)-\tfrac{1}{2}(A^2+B^2)^2]+4\pi^2[1+2\varepsilon\cos(\vartheta)+\varepsilon^2](A^2+B^2)+\left(\frac{\partial A}{\partial x}\right)^2+\left(\frac{\partial A}{\partial z}\right)^2\right]+\int\int dx\,dz\left\{\left(\frac{\partial B}{\partial x}\right)^2+\left(\frac{\partial B}{\partial z}\right)^2+4\pi\left[\sin(\vartheta)\left(\frac{\partial A}{\partial x}B-\frac{\partial B}{\partial x}A\right)+[\cos(\vartheta)+\varepsilon]\left(\frac{\partial A}{\partial z}B-\frac{\partial B}{\partial z}A\right)\right]\right\}+\int\int dx\,dz\left\{\frac{q_b^2\lambda^2}{2}\left[\left(\frac{\partial\vartheta}{\partial x}\right)^2+\left(\frac{\partial\vartheta}{\partial z}\right)^2\right]\right\}+\int\frac{d_b}{2\zeta}[(A-A_s)^2+(B-B_b)^2]dz. \tag{3b}$$

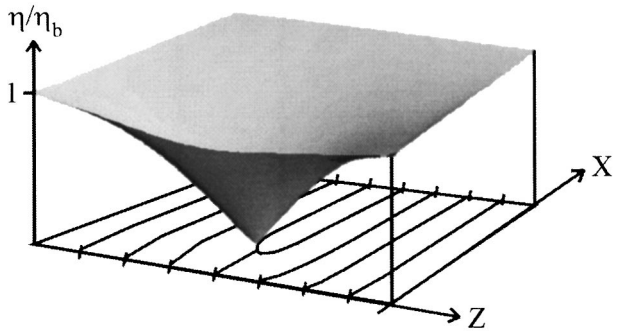

FIG. 3. The spatial profile $\eta=\eta(x,z)$ of the smectic order parameter superimposed on the corresponding layer structure for $U=10U_m$. $\tau=-0.05$, $\varepsilon=0.05$, and $U_m=0.5$.

The relevant dimensionless parameter corresponding to the surface properties is the ratio $U=d_b/\zeta=W_p d_b/\gamma$. This quantity characterizes the dislocation formation properties of the system. We also make the simplifying approximation that the surface and bulk degree of smectic ordering are equal ($\eta_s=\eta_b$). This approximation does not affect the qualitative behavior of the model.

We focus on the case of a semi-infinite cell where $L_x\to\infty$. Phenomena at opposite plates are now decoupled. The results we present thus now concern an idealized case in which there is mismatch between bulk periodicity and surface periodicity on one plate placed at $x=0$. The relevant Euler-Lagrange equations have been solved numerically, using the overrelaxation method [14].

III. RESULTS

A. Formation and depinning

We first consider the structure of an edge dislocation in the strong positional anchoring limit (i.e., $U=\infty$). In this case, the surface strongly enforces periodicity q_s at the bounding plate. In order to obtain bulk smectic ordering with periodicity q_b far from the surface, a lattice of edge dislocations must necessarily be formed at a finite distance r from the surface. In Fig. 3, we show the corresponding spatial variation of the smectic order parameter $\eta(x,z)$. At the center of each edge dislocation, the smectic phase melts and the ordering disappears as a result of topological requirements.

The core region, where the smectic degree of ordering apparently departs from the bulk value η_b, is asymmetric (note that calculations are carried for $\gamma_\parallel=\gamma_\perp\equiv\gamma$). Only far from the surface does the smectic ordering recover the bulk degree of ordering; it does so on a length scale of the order of the smectic correlation length. Even at the defect site, the

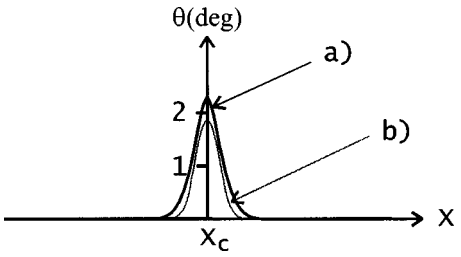

FIG. 4. The director field departures from the bookshelf arrangement at the dislocation core in comparison to the results of the standard harmonic approach [1] in terms of a scalar displacement field. The defect is placed at *x*. (a) Landau–de Gennes and (b) harmonic approach.

nematic director field exhibits only a negligible departure from the *z* direction. These departures are shown in Fig. 4. Following this result, we feel confident in constraining **n** to be along the *z* direction in all subsequent calculations.

In the same figure, we also compare the core structure obtained within our approach with the one resulting from the standard continuum approach [1,4] where LC molecules are locked along the layer normal and the cutoff radius is introduced at the defect. For the example shown, the departures are relatively small.

In the semi-infinite geometry, the local surface structure is a function of the two dimensionless parameters ε and U. Here we focus on the formation and evolution of edge dislocations at constant strain. A full spectrum of behaviors occurs as the surface positional anchoring strength is changed.

For $U=0$, the smectic layers adopt the undistorted bookshelf structure. The phase favored by the local surface is unable to influence the phase close to the surface because of the zero coupling. As the surface anchoring parameter U increases from zero, the smectic layers deform. In this regime, the average layer periodicity is given by the bulk periodicity. However, due to the surface coupling, the layering near the surface tries to follow the surface-favored periodicity, but is unable to do so. The net effect, near the surface, is to cause regions in which the local layering seems locked onto the surface-favored structure, separated by phase-jump regions that realign the layer periodicity with the bulk.

Equivalently, near the surface the phase factor exhibits a solitonlike profile in the *z* direction. The surface-induced distortions persist away from the surface over a distance determined by ξ and ε. In the limit $x \gg \xi$, the undistorted smectic bookshelf structure is recovered.

Let us focus on the region close to the surface. At the soliton wall—defined as the site of maximal φ variation—the surface and bulk layers are out of phase. This affects the magnitude of the smectic order parameter in this region, which is reduced. The quantity $\eta(0,z)$ reaches a minimum $\eta_{\min}$ at the soliton wall. This is shown in Fig. 5(a).

As the smectic anchoring U is increased, the value of $\eta_{\min}$ decreases in a roughly linear fashion. At a threshold value $U=U_m(\varepsilon,\tau)$, the stress imposed on the smectic layers is sufficiently strong that $\eta_{\min}$ reaches zero. The smectic melts

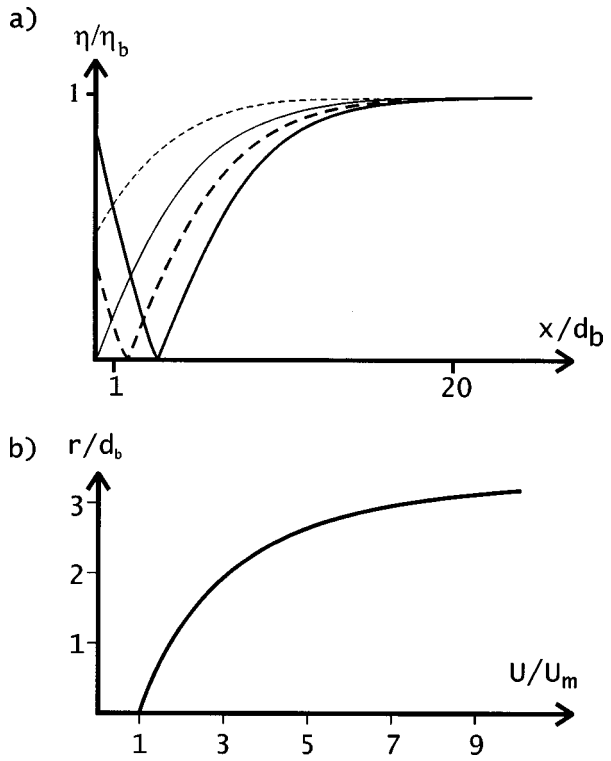

FIG. 5. (a) The spatial variation of η in the *x* direction at the soliton wall for $|\varepsilon|=0.05$, $\tau=-0.05$, and different values of U ($U/U_m=0.5,1,3,7$). (b) The position r of the edge dislocation as a function of U/U_m.

at the surface, and there are now edge dislocations located precisely at the surface.

Then as U is increased beyond its critical value U_m, the dislocations *depin* from the surface, apparently continuously. As U is increased further, the defect is now repelled from the surface. The surface region is now dominated by the surface periodicity. In this regime, the mismatch between the surface and bulk periodicities is relieved by a lattice of defects located at a distance $r=r(U,\varepsilon,\tau)$ from the boundary. The behavior of the distance r of the edge dislocation as a function of U is shown in Fig. 5(b). We note that for $U \gg U_m$, the dislocation asymptotically approaches a fixed distance r from the surface. We find numerically that, roughly speaking, $r \propto 1/|\varepsilon|$.

Finally, we have numerically determined the critical value $U_m(\varepsilon,\tau)$. We find linear behavior, roughly given by

$$U_m(\varepsilon,\tau) \sim 0.08 + 5.2|\varepsilon| - 3.2\tau. \tag{4}$$

As expected, the threshold smectic anchoring for dislocation formation is lower close to the *N*-Sm*A* phase transition.

B. Determination of W_p

The formation of edge dislocations in the case we have studied strongly depends on the surface coupling W_p. This coupling also plays an important role in various electro-optic

applications. Normally, we expect a high W_p to favor the formation of (in principle unwanted) chevron structures in surface-stabilized ferroelectric cells. Therefore, it is of interest to know its strength in order to predict possible effects it can cause. Despite its importance for various electro-optic applications, the only known estimate of W_p has hitherto been reported by Cagnon and Durand [7]. Using a micromechanical technique, they measured W_p for the Sm*A* LC 40.8 yielding a value $W_p \sim 10^{-8}$ J/m^2. Such an extremely low value of W_p is from our point of view rather surprising in view of the conventional view that strong memory effects pin the surface layers.

We now propose a possible determination of W_p using the edge-dislocation depinning process discussed in this paper. We analyze the simplest possible scenario from the experimental point of view. For this reason, we study the surface-induced formation of a lattice of edge dislocations. The temperature of a liquid crystal in the Sm*A* phase is increased starting from the defectless state.

We take advantage of the strong τ dependence of $U_m = U_m(\tau)$ found in our numerical study. By contrast, experiments [11] indicate a relatively weak temperature dependence of ε. Assuming temperature-independent values of U and ε, there will now be a temperature-driven transition from the defect-free state at $U < U_m$ into a $U > U_m$ regime where dislocations do occur. We have numerically examined the case $U = 0.25$ and $\varepsilon = 0.01$ and the temperature is increased from $\tau = \tau_1$ to τ_2. Initially, the system is in the distorted bookshelf structure where $U < U_m(\tau_1) = 0.3$ and $(\tau_1 = -0.05)$ [see Eq. (4)]. The Sm*A* phase is then heated to $\tau_2 = -0.01$, where now the condition is $U > U_m(\tau_2) = 0.17$. For a typical Sm*A* liquid crystal, one finds $\gamma \sim 10^{-12}$ J/m^2, $d_0 \sim 2$ nm. In this case, the phenomenon is observable if $T_1 \sim T_{NA} - 30$ K, $T_2 \sim T_{NA}$, and $W_p \sim 10^{-4}$ J/m^2. Thus the effective surface anchoring can be tuned by changing the temperature, and the dislocation lattice can be induced by a temperature change.

There are two main obstacles from the experimental point of view to realize the proposed scenario experimentally. First, the depinning process only weakly affects nematic orientational ordering, excluding the use of relatively simple optic methods. An experimental method that directly probes the smectic layers is therefore needed. We believe that x-ray scattering localizing the scattering close to an enclosing cell plate (the penetration length of few smectic correlation lengths is favorable) is adequate for this purpose. In this case, the appearance of edge dislocations would result in the broadening of the scattering spectrum.

The second problem concerns the condition $d_b/d_s > 1$, in which edge dislocations are likely to appear. In practice, this condition occurs only rarely. The mismatch normally appears as a result of the memory effect, in which case $d_b/d_s < 1$. In this case, for most materials and reasonable values of L_x, the chevron structure is usually observed [6,9,11]. The chevron structure can be avoided by applying an external electric or magnetic field sustaining the bookshelf alignment (i.e., $\vartheta = 0$). In the chevron structure, the LC molecules are on average tilted for $\vartheta_c \sim \arccos(d_b/d_s)$ [6,9]. This subsequently causes a strong free-energy penalty proportional to the cell thickness L_x.

We can estimate the critical electric field required to stabilize the dislocation structure. The idea is to compare the free energy F cost of the chevron (F_c) and the ''dislocation'' (F_d) structure (i.e., the structure incorporating a lattice of defects). The electric field E is supposed to be aligned along the z direction. In the chevron structure, the director field reorients from $\vartheta(x=0) = 0$ to $\vartheta_c \sim \arccos(d_b/d_s) \sim \sqrt{2\varepsilon}$ at a distance given by the smectic penetration length λ. The relevant free-energy cost F_c of this configuration is $F_c/KL_y \sim L_z((\vartheta_c^2/2\lambda) - [(L_x \cos^2 \vartheta_c)/2\xi_E^2])$, where $\xi_E = \sqrt{K/\Delta\varepsilon\varepsilon_0 E^2}$ is the field correlation length. The first term estimates the nematic elastic costs at the surface and the second is the field contribution.

In the dislocation structure, we assume that the main contributions come from the melted regions at defect sites that roughly occupy the volume $\pi L_y \xi^2 N_{\text{edge}}$. Here $N_{\text{edge}} \sim \varepsilon L_z/d_b$ [6] estimates the number of edge dislocations at one surface. With this in mind, we obtain $F_d/KL_y \sim L_z[(\pi\gamma\eta^2\varepsilon/2Kd_b) - (L_x/2\xi_E^2)]$.

The dislocation structure is preferred to the chevron structure if $F_d < F_c$, yielding the following condition:

$$\frac{L_x d_b}{\xi_E^2} > \frac{\pi}{2q_0^2\lambda^2} - \frac{d_b}{\lambda}. \tag{5}$$

Thus the threshold external field necessary to stabilize the dislocation structure is proportional to $1/\sqrt{L_x}$.

Note that the presence of an external field supporting the bookshelf structure does not affect our calculations. The external field is strongly coupled only to the director field. This has practically the same configuration in the dislocation structure with or without the external field.

IV. CONCLUSIONS

We have studied surface-induced formation and depinning of an edge dislocation in a Sm*A* phase by means of a Landau–de Gennes description. A simple surface positional anchoring term is proposed in order to study the competition between bulk elastic and surface forces. Edge dislocations are the consequence of the mismatch between surface and bulk periodicities.

We have studied the onset of an edge dislocation by increasing the surface positional anchoring strength U. We show that with increased U, the edge dislocation is formed at the surface and then depinned from it in a continuous way. The critical condition for the edge-dislocation formation has been obtained numerically. For a large enough value of U, an edge dislocation saturates at a finite distance r from the surface. In the regime we have studied, we find $r \propto 1/|\varepsilon|$.

We have then used our picture of dislocation depinning to provide a possible experimental route toward measuring W_p. To the best of our knowledge, only one measurement [7] of this constant has been reported, suggesting a suprisingly low value $W_p \sim 10^{-8}$ J/m^2. The experimental observation of the

proposed scenario can serve as a test of this prediction or can at least yield the upper limit of W_p values.

In future work, we will study the influence of the cell thickness L_x on the dislocation lattice structure within the cell. Our preliminary studies show that phenomena at both plates strongly interfere when the cell thickness becomes comparable to the smectic correlation length. For even smaller values of L_x, the interacting edge dislocations at different plates may annihilate, once again forming a defect-free structure.

ACKNOWLEDGMENTS

This research was supported by a bilateral cooperation between Italy and Slovenia. We thank L. D. Hazelwood and G. Durand for an illuminating discussion.

[1] P. G. de Gennes and J. Prost, *The Physics of Liquid Crystals* (Oxford University Press, Oxford, 1993).
[2] M. Kleman, *Points, Lines and Walls* (Wiley, Chichester, 1983).
[3] S. R. Renn and T. C. Lubensky, Phys. Rev. A **38**, 2132 (1988).
[4] E. B. Loginov and E. M. Terentjev, Kristallografiya **32**, 288 (1987) [Sov. Phys. Crystallogr. **32**, 166 (1987)].
[5] S. Kralj and T. J. Sluckin, Liq. Cryst. **18**, 887 (1995).
[6] S. Kralj and T. J. Sluckin, Phys. Rev. E **50**, 2940 (1994).
[7] See M. Cagnon and G. Durand, Phys. Rev. Lett. **70**, 2742 (1993) for a measurement of the effective surface potential.
[8] See A. N. Shalaginov, L. D. Hazelwood, and T. J. Sluckin, Phys. Rev. E **58**, 7455 (1998) for an alternative dynamic paradigm for the memory effect. However, even from this viewpoint, an effective surface layer anchoring should be definable.
[9] See, e.g., L. Limat and J. Prost, Liq. Cryst. **13**, 101 (1993).
[10] N. A. Clark, T. P. Rieker, and J. E. Maclennan, Ferroelectrics **85**, 79 (1988).
[11] Y. Ouchi, Y. Takanishi, H. Takezoe, and A. Fukuda, Jpn. J. Appl. Phys., Part 1 **28**, 2547 (1989).
[12] M. Slavinec, S. Kralj, and S. Žumer (unpublished).
[13] E. B. Loginov and E. M. Terentjev, Kristallografiya **30**, 10 (1985) [Sov. Phys. Crystallogr. **30**, 4 (1985)].
[14] F. J. Vesely, *Computational Physics* (Plenum Press, New York, 1994).